

# Alkane Lengths Determine Encapsulation Rates and Equilibria

Wei Jiang, Dariush Ajami, and Julius Rebek, Jr.\*

The Skaggs Institute for Chemical Biology and Department of Chemistry, The Scripps Research Institute, 10550 North Torrey Pines Road, La Jolla, California 92037, United States

**S** Supporting Information

**ABSTRACT:** A cylindrical capsule provides an environment for straight-chain alkanes that can properly fill the space through extended or compressed conformations. The encapsulation rates of a series of alkanes were examined and found to be dependent on guest length: the rates of uptake are  $C_9 > C_{10} > C_{11}$ , while complex stability is in the reverse order,  $C_{11} > C_{10} > C_9$ . Direct competition experiments, pairwise or between all 3 alkanes, maintain this order as the longer alkanes sequentially displace the shorter ones. The distribution of species with time provides a clock for this complex system, which combines elements of self-sorting phenomena and dynamic combinatorial chemistry. The clock can be stopped by replacing the alkanes with the superior guest 4,4'-dimethylazobenzene, then restarted by irradiation.

Multicomponent host/guest systems increase the complexity of supramolecular chemistry from simple binary or ternary combinations to molecular networks that can be analyzed at the systems level.<sup>1</sup> For example, dynamic combinatorial chemistry<sup>2</sup> allows the synthesis of the otherwise inaccessible molecular architectures of structural complexity<sup>3</sup> while self-sorting phenomena<sup>4</sup> are driven by relatively well-understood thermodynamic properties. Related networks in nature are highly complex and dynamic with exchanging binding partners or changing conformations.<sup>5</sup>

Self-assembled capsules<sup>6</sup> are reversibly formed assemblies that can surround their guests and isolate them from each other and the bulk solution. The capsules can act as molecular flasks to catalyze or control reactions,<sup>7</sup> behave as containers to stabilize reactive intermediates,<sup>8</sup> and often amplify intermolecular interactions.<sup>9</sup> The guest exchange rates define the lifetimes of the encapsulation complexes, which lifetimes range from milliseconds to days.<sup>10</sup> Although pairwise competition has been widely studied,<sup>11</sup> complex kinetic behaviors of guest exchange in capsule are rarely studied in the context of complex networks, that is, at the systems level.<sup>12</sup> The cylindrical capsule **1.1**<sup>13</sup> (Figure 1a) features a nonspherical inner space, which can accommodate long, narrow, and flexible guests such as *n*-alkanes.<sup>14</sup> The exchange rates of a single, long guest are much slower than small guest pairs,<sup>15</sup> and we show here that the exchange of *n*-alkane guests exhibits sequence-specific kinetics.

The *n*-alkanes from  $C_9$  to  $C_{14}$  are all good guests for the cylindrical capsule **1.1** but assume different shapes inside: extended (for  $C_9$ ,  $C_{10}$ , and  $C_{11}$ ) or coiled (for  $C_{12}$ ,  $C_{13}$ , and  $C_{14}$ ) conformation. The absolute binding constants ( $>10^8 \text{ M}^{-2}$ ) are too high to be measured since the free cavitand is not

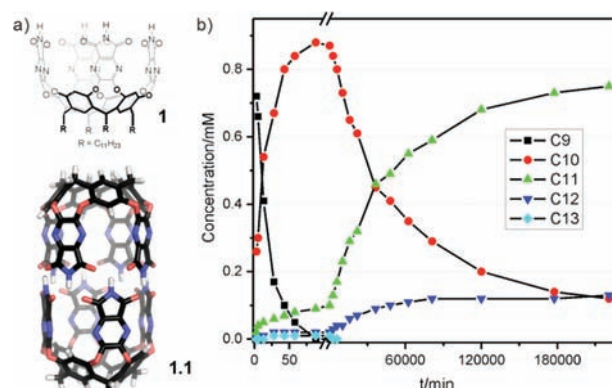


**Figure 1.** (a) Chemical structure of cavitand **1** and its dimeric capsule **1.1**. (b) Concentration changes (mesitylene- $d_{12}$ , 300 K) of encapsulated guests as a function of time after adding a mixture of six *n*-alkanes ( $C_9$ ,  $C_{10}$ ,  $C_{11}$ ,  $C_{12}$ ,  $C_{13}$ , and  $C_{14}$ ; 30 equiv each) to a solution of **1.1** (1.0 mM).

detectable by  $^1\text{H}$  NMR, but relative binding constants among the *n*-alkanes are available from the earlier studies,<sup>14</sup> which are reconfirmed and corrected by this research (see Table 1 and

**Table 1. Rate Constants and Half-Lives<sup>21</sup> for Exchange of Capsule Halves with *n*-Alkanes as the Guests in **1.1**, and Relative Binding Affinities,<sup>14</sup> Relative Free Energies and Packing Coefficients of *n*-Alkanes in **1.1****

guest	$k_{-1}$ ( $\text{s}^{-1}$ )	$t_{1/2}$	$K_{\text{rel}}$	$\Delta\Delta G^\circ$ (300 K, $\text{kJ mol}^{-1}$ )	PC
<i>n</i> -nonane ( $C_9$ )	$1.6 \times 10^{-3}$	7 min	0.3	3.0	43
<i>n</i> -decane ( $C_{10}$ )	$5.4 \times 10^{-6}$	36 h	16.9	-7.1	48
<i>n</i> -undecane ( $C_{11}$ )	$\ll 2 \times 10^{-6}$	$\gg 100$ h	100	-11.5 (0 gauche) <sup>18</sup>	52
<i>n</i> -dodecane ( $C_{12}$ )	$3.8 \times 10^{-6}$	51 h	24.4	-8.0 (4 gauche) <sup>18</sup>	54
<i>n</i> -tridecane ( $C_{13}$ )	$8.1 \times 10^{-6}$	24 h	1.0	0.0 (8 gauche) <sup>18</sup>	55
<i>n</i> -tetradecane ( $C_{14}$ )	$6.8 \times 10^{-6}$	28 h	0.008	12.0 (11 gauche) <sup>18</sup>	58

Figure S1 in Supporting Information (SI)). The binding stability goes up from  $C_9$  to  $C_{11}$ , peaks at  $C_{11}$ , and then decreases from  $C_{11}$  to  $C_{14}$ .<sup>16</sup> This indicates  $C_{11}$  is the best fit for the cavity of capsule **1.1**. The coiled conformation assumed by

Received: March 19, 2012

Published: May 1, 2012

the longer alkanes creates *gauche* interactions along the backbone and exerts pressure on the inside of the capsule. The thicker coiled hydrocarbon can make more C–H/ $\pi$  contacts with the capsule but these attractions do not appear to compensate for the destabilizing aspects and overall lead to weaker binding of the compressed alkanes.<sup>17</sup> The relative affinities and free energies of the hydrocarbon complexes in Table 1 show a large price is paid by the weakest binder, C<sub>14</sub>. This guest requires 11 *gauche* conformations to fit while C<sub>13</sub> requires 8 *gauche* conformations.<sup>18</sup> The relative affinity of C<sub>14</sub>/C<sub>13</sub> is 0.008. The value reported in ref 14 (13.2) is incorrect, probably due to measurement before equilibration. Given the value recommended by Eliel<sup>19</sup> for a *gauche* effect in the liquid state (0.54–0.57 kcal mol<sup>-1</sup>; 2.3–2.4 kJ mol<sup>-1</sup>), the different stabilities of the complexes with C<sub>14</sub>/C<sub>13</sub> (12 kJ mol<sup>-1</sup>) is attributed to both the additional 3 *gauche* interactions (6.9–7.2 kJ mol<sup>-1</sup>) and the pressure exerted on the capsule.<sup>17</sup> The 100-fold C<sub>13</sub>/C<sub>11</sub> stability ratio reveals the full cost of compression of C<sub>14</sub> (maximally coiled) versus C<sub>11</sub> (fully extended) as 23.5 kJ mol<sup>-1</sup>. For 11 *gauche* interactions, the value is expected to be 25.3–26.4 kJ mol<sup>-1</sup>. If the solvation/desolvation energy differences between C<sub>11</sub> and C<sub>14</sub>, free in solution, are included, the encapsulation of C<sub>14</sub> should be even less favorable. However, the binding data may reflect the stabilizing contributions of C–H/ $\pi$  interactions.<sup>20</sup>

The exchange rates of capsule halves in the presence of *n*-alkanes have been studied in real time by FRET experiments.<sup>21</sup> Their half-lives are guest-dependent and range from 7 min for C<sub>9</sub> to more than 100 h for C<sub>11</sub> (see Table 1). Although guest exchange might not require dissociation of the two capsule halves, the data of Table 1 is consistent with this mechanism: from C<sub>9</sub> to C<sub>11</sub>, the capsule dissociation rate decreases. Therefore, the kinetic stabilities of C<sub>9</sub>, C<sub>10</sub>, and C<sub>11</sub> are in the reverse order of their thermodynamic stabilities. This suggested that when mixing these *n*-alkanes with the free (i.e., solvent impurity-filled) capsule, a sequential kinetic pattern would be observed over time.

An initial kinetic experiment was performed by adding a mixture of six *n*-alkanes (C<sub>9</sub>–C<sub>14</sub>) to the solution of the capsule 1.1 and monitoring by <sup>1</sup>H NMR (Figure S2). The concentration changes of each encapsulated guests as a function of time are shown in Figure 1b. The following observations are clear. (a) At the beginning, the capsule was predominantly occupied by C<sub>9</sub>. (b) During the first 100 min, C<sub>9</sub> gradually ceded the capsule to C<sub>10</sub>. Although C<sub>12</sub> and C<sub>13</sub>-occupied capsules were detected, they remained at very low concentrations. (c) On a longer time scale, the encapsulated C<sub>10</sub> was further displaced by C<sub>11</sub>, but very slowly. The concentration of C<sub>12</sub> in the capsule also increased slightly, but the encapsulated C<sub>13</sub> quickly disappears. Clearly, a sequence-specific kinetic uptake of C<sub>9</sub>, C<sub>10</sub>, and then C<sub>11</sub> by capsule 1.1 occurs. This is even clearer if only these three *n*-alkanes are used as the guests to exclude the interference of C<sub>12</sub> (see Figures S3, S4).

We further checked the sequential displacement of these *n*-alkanes by deliberately providing some assembly “errors” in this system. Initially, the least stable *n*-alkane C<sub>14</sub> was encapsulated and then the mixture of the other five *n*-alkanes (C<sub>9</sub>–C<sub>13</sub>) was added to the solution (Figure S5). The assembly error was corrected again through the sequence C<sub>9</sub> → C<sub>10</sub> → C<sub>11</sub>. The same was true for the two other possible “errors” with C<sub>12</sub> or C<sub>13</sub>-occupied capsules as the initial states (Figures S6, S7), although the intermediate state with C<sub>9</sub> in the capsule was not observed.

The displacement of the encapsulated C<sub>10</sub> by C<sub>11</sub> appears to be extremely slow, requiring more or less 3 months to complete. We speculate that C<sub>10</sub> represents a kinetic trap here. To bypass this kinetic trap, a mixture of five *n*-alkanes (C<sub>9</sub> and C<sub>11</sub>–C<sub>14</sub>) excluding C<sub>10</sub> was added to the solution of capsule 1.1 and the kinetic evolution of each encapsulated species was monitored (Figures S8, S9). Indeed, the rates were much faster than in the presence of C<sub>10</sub>. But more assembly errors—encapsulated C<sub>12</sub> and C<sub>13</sub>—were observed at the beginning then decreased or disappeared shortly. To some extent, this weakens the sequence-specificity; C<sub>10</sub> slows down the overall kinetics but it does maintain the kinetic sequence by prohibiting the kinetic errors of encapsulated C<sub>12</sub> and C<sub>13</sub>.

What is the guest exchange mechanism? Earlier studies<sup>15</sup> with rigid single guests or guest pairs in 1.1 support a gating mechanism<sup>22</sup> whereby one or two walls open to allow guest displacement. Two further refinements for this mechanism exist:<sup>10</sup> the first one is in analogy to S<sub>N</sub>1 reaction by involving a state where the resident guest has departed but the incoming guest has not yet arrived (an intermediate); the second is an S<sub>N</sub>2-like substitution with the incoming guest forcing out the resident.

As shown in Figure 2, the initial rate of C<sub>9</sub> displaced by C<sub>11</sub> was directly proportional to the concentration of C<sub>11</sub> at low

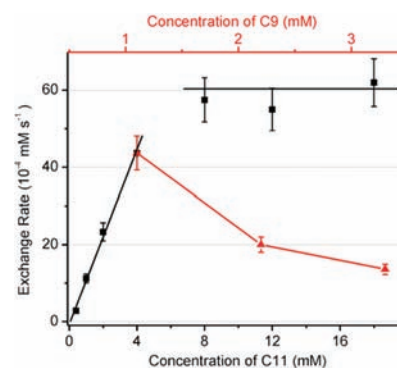


**Figure 2.** Rates of the displacement C<sub>9</sub> → C<sub>11</sub> as a function of the concentration of the incoming guest C<sub>11</sub> (black ■) with fixed [C<sub>9</sub>] = 1.1[1.1] = 1.1 mM and as a function of the total concentration of the outgoing guest C<sub>9</sub> (red ▲) with fixed [C<sub>11</sub>] = 4[1.1] = 4.0 mM.

[C<sub>11</sub>] but levels off at high [C<sub>11</sub>]. This saturation kinetics indicate a pre-equilibrium in the mechanism before C<sub>11</sub> is involved, that is, an intermediate exists prior to the encapsulation of C<sub>11</sub>. What is the nature of this intermediate? Apparently, the intermediate *has lost the resident guest* because there is an inverse dependence of exchange rate on the concentration of added, (free) outgoing guest C<sub>9</sub> (Figure 2). This is similar to the exchange mechanism of rigid guests.<sup>15</sup> It is unlikely that the intermediate is an empty capsule. Rather, solvent molecules or solvent impurities such as benzene or *p*-xylene could occupy the capsule in the intermediate state. To further replace these occupants by the incoming guests and complete the guest exchange process, a S<sub>N</sub>2-like mechanism may be invoked.<sup>23</sup>

Under pseudo zero-order conditions for outgoing and incoming guests, the displacement kinetics show zero-order dependence on the concentration of outgoing guest occupied capsule during the reaction (Figures S12–S20). This suggests that either a catalyst saturated by the substrate (the outgoing guest occupied capsule) is involved prior to the rate-

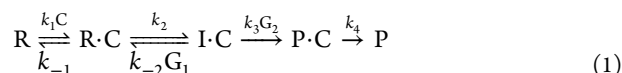
determining step (rds) or reaction with the substrate occurs after the rds. The latter can be ruled out since the rates shows reverse dependence on the concentration of outgoing guest. That is, a catalyst should be involved which is meanwhile saturated by the substrate. This is supported by the curved zero-order kinetics at the later stage of exchange when the substrate at low concentration cannot saturate the catalyst. In addition, the exchange rates are shown to be proportional to the initial concentration of capsule, suggesting the catalyst probably is associated with cavitand **1**. Free cavitand **1** may be a good candidate, but it is in equilibrium with the capsule and a different capsule or capsule composition should lead to different concentrations of free **1**. If the catalyst is **1**, we should expect the dependence of rates on capsule composition to change during the displacement but that is not the case. Instead, we propose the catalyst(s) are hydrogen-bonding impurities such as H<sub>2</sub>O, cavitand wall, or MeOH (Figures S22–S24), all of which accelerate the substitution reactions. During the reaction, a “broken” capsule with two dissociated halves may be involved when releasing C<sub>9</sub>. This is in line with the longer half-lives (>19 min, Table 2) for guest displacement than those for exchange of capsule halves (7 min for C<sub>9</sub>, Table 1).

**Table 2. Observed Rate Constants, Half-Lives, and the Relative Activation Energies for Pairwise Guest Exchange**

	$k_{\text{obs}}$ (mM s <sup>-1</sup> )	$t_{1/2}$	$\Delta\Delta G^\ddagger$ (300 K, kJ mol <sup>-1</sup> )
C <sub>9</sub> → C <sub>10</sub>	$(4.5 \pm 0.50) \times 10^{-4}$	19 min	6.5 <sup>a</sup>
C <sub>9</sub> → C <sub>11</sub>	$(7.3 \pm 0.70) \times 10^{-5}$	1.9 h	11.0 <sup>a</sup>
C <sub>9</sub> → C <sub>12</sub>	$(3.4 \pm 0.30) \times 10^{-5}$	4.1 h	12.9 <sup>a</sup>
C <sub>9</sub> → C <sub>13</sub>	$(3.2 \pm 0.40) \times 10^{-5}$	4.4 h	13.1 <sup>a</sup>

<sup>a</sup> $\Delta\Delta G^\ddagger$  of (I) → G<sub>2</sub> ( $k_3$ ) was calculated relative to the activation barrier of (I) → C<sub>9</sub> ( $k_{-2}$ ).

With all the evidence above, the guest displacement mechanism can be summarized in the following eq 1:



Under the present experimental conditions, the catalyst (C) is “saturated” and thus  $[\text{R}\cdot\text{C}] \approx [\text{C}]_0$ . The data in Table 2 shows that the step involving the incoming guest (G<sub>2</sub>) controls the overall rate and is the rds. On treating the subsequent reactions with the steady-state approximation, we obtain

$$\frac{d[\text{P}]}{dt} = \frac{k_3[\text{G}_2]k_2[\text{C}]_0}{k_{-2}[\text{G}_1] + k_3[\text{G}_2]} \quad (2)$$

This equation is in agreement with the saturation kinetics observed in Figure 2. Under the conditions  $[\text{G}_1] = [\text{G}_2] \gg [1.1]$  and  $k_{-2} \gg k_3$  (when C<sub>9</sub> is the outgoing guest (G<sub>1</sub>)), the eq 2 can be simplified into:

$$\frac{d[\text{P}]}{dt} = \frac{k_3k_2[\text{C}]_0}{k_{-2}} = k_{\text{obs}} \quad (3)$$

Therefore, a zero-order rate law can be used to analyze the kinetic data. With the data (Table 2 and S1) on pairwise competition, we arrive at the specific encapsulation sequence (C<sub>9</sub> → C<sub>10</sub> → C<sub>11</sub>). Table 2 lists the displacement rates of the encapsulated C<sub>9</sub> by the more stable guests. The data shows that C<sub>10</sub> was the fastest to displace C<sub>9</sub>, followed by C<sub>11</sub>, and then C<sub>12</sub>

and C<sub>13</sub>. When C<sub>10</sub> occupies the capsule, C<sub>11</sub> displaces it more quickly than C<sub>12</sub> (Table S1), and the sequence-specific kinetics can be understood: (a) C<sub>9</sub> was the fastest guest to occupy the capsule; (b) C<sub>10</sub> is the fastest guest to displace C<sub>9</sub>; (c) only two guests can displace C<sub>10</sub> for thermodynamic reasons, but C<sub>11</sub> is faster and also a more stable guest than C<sub>12</sub>; (d) both the relative rates and relative stabilities play important roles in determining the C<sub>9</sub> → C<sub>10</sub> → C<sub>11</sub> encapsulation sequence.

The relative activation energies were also determined. The eq 3 can be rearranged into:

$$\frac{k_3}{k_{-2}} = \frac{k_{\text{obs}}}{k_2[\text{C}]_0} \quad (4)$$

and  $k_2[\text{C}]_0$  ( $\approx 6.0 \times 10^{-3}$  mM s<sup>-1</sup>) with C<sub>9</sub> as outgoing guest can be obtained from the saturation kinetics (Figure 2) when  $k_3[\text{C}_{11}] \gg k_{-2}[\text{C}_9]$ . Using the Eyring equation and the data in Table 2, the activation free energy of (I) → G<sub>2</sub> ( $k_3$ ) relative to that of (I) → C<sub>9</sub> ( $k_{-2}$ ) can be calculated directly. The results are listed in Table 2. With increasing the length of the *n*-alkanes, the relative activation free energies also increase. But the increase diminishes for longer alkane. This trend was confirmed by the analysis of the activation data (Table S2). The activation barrier difference appears to be mainly enthalpic in origin (Table S3). The increased activation barriers with longer guests may arise from breaking more hydrogen-bonds to create larger openings. Since longer guests require more solvation, the desolvation of free guest should also contribute to the activation energy. Clearly, hydrogen-bond breaking does occur in the transition state, which is verified by the accelerated exchange kinetics on addition of molecules rich in hydrogen-bond donors and acceptors, for example, bis-(*N,N'*-dibutylphenyl)glycouril (**2**) and MeOH (Figures S22–S24).

In addition, this sequence-specific kinetic behavior is not limited to the system with the *n*-alkane guests and the cylindrical capsule **1.1**. Replacing *n*-alkane guests with *n*-alkyl aldehyde guests or using glycouril-extended capsule **1.24.1** instead of **1.1** results in similar guest-length dependent kinetic behavior (Figures S25, S26), although the kinetic sequence is not as clear-cut as for **1.1**.

By incorporating a photoswitchable guest 4,4'-dimethylazobenzene (Azo),<sup>24</sup> the kinetic system with three essential alkanes (C<sub>9</sub>, C<sub>10</sub>, and C<sub>11</sub>) and capsule **1.1** can be “reset”. *Trans*-Azo can replace alkane guests by boiling the solution for ca. 30 s (boiling point of mesitylene: 165 °C), then cooling to room temperature (Figure S27). Under photoirradiation at 365 nm for 30 min, *trans*-Azo isomerizes; the *cis*-Azo breaks out of the capsule,<sup>24</sup> and the competition of the alkanes for encapsulation starts again. Regardless of the initial conditions, the sequence-specific guest exchange can be stopped or reset by boiling the solution then photoirradiating it (Figures S28, S29).

In summary, a sequence-specific pathway was identified during encapsulation of a small library of *n*-alkane guests in **1.1**. This system is readily reset by incorporating an azobenzene guest through heating and photoirradiation. In analogy to guest exchange kinetics of the “softball”,<sup>23</sup> an S<sub>N</sub>1-like mechanism was supported for the displacement process. The systematic elongation of *n*-alkane guests gradually increases their displacement/assembly activation barriers, but the binding energies first increase and then decrease with length. An intricate interplay of kinetics and thermodynamics determines this encapsulation pathway (C<sub>9</sub> → C<sub>10</sub> → C<sub>11</sub>). In this system, error-correction occurs in a highly specific sequence and both the ingredients of

kinetic self-sorting and dynamic combinatorial chemistry exist. Parallels in nature exist in enzymes<sup>25</sup> where substrates smaller than the cognates may react faster, but are corrected by the editing functions.

## ■ ASSOCIATED CONTENT

### 📄 Supporting Information

Experimental procedures, rate-constant determinations, Arrhenius plots, Tables S1–S3, and Figures S1–S29. This material is available free of charge via the Internet at <http://pubs.acs.org>.

## ■ AUTHOR INFORMATION

### Corresponding Author

jrebek@scripps.edu

### Notes

The authors declare no competing financial interest.

## ■ ACKNOWLEDGMENTS

We thank the Skaggs Institute for Chemical Biology and NSF (NSF/CHE 1037590) for financial support and Prof. Stephen L. Craig for stimulating interpretations and advice. W.J. is a Skaggs Postdoctoral Fellow.

## ■ REFERENCES

- (1) Ludlow, R. F.; Otto, S. *Chem. Soc. Rev.* **2008**, *37*, 101.
- (2) (a) Lehn, J.-M. *Chem.—Eur. J.* **1999**, *5*, 2455. (b) Rowan, S. J.; Cantrill, S. J.; Cousins, G. R. L.; Sanders, J. K. M.; Stoddart, J. F. *Angew. Chem., Int. Ed.* **2002**, *41*, 898. (c) Corbett, P. T.; Leclaire, J.; Vial, L.; West, K. R.; Wietor, J.-L.; Sanders, J. K. M.; Otto, S. *Chem. Rev.* **2006**, *106*, 3652.
- (3) Cougnon, F. B. L.; Sanders, J. K. M. *Acc. Chem. Res.* **2012**, DOI: 10.1021/ar200240m.
- (4) Safont-Sempere, M. M.; Fernández, G.; Würthner, F. *Chem. Rev.* **2011**, *111*, 5784.
- (5) Aderem, A. *Cell* **2005**, *121*, 511–513.
- (6) Hof, F.; Craig, S. L.; Nuckolls, C.; Rebek, J., Jr. *Angew. Chem., Int. Ed.* **2002**, *41*, 1488–1508.
- (7) Yoshizawa, M.; Klosterman, J. K.; Fujita, M. *Angew. Chem., Int. Ed.* **2009**, *48*, 3418–3438.
- (8) For examples: (a) Iwasawa, T.; Hooley, R. J.; Rebek, J., Jr. *Science* **2007**, *317*, 493–496. (b) Kawamichi, T.; Haneda, T.; Kawano, M.; Fujita, M. *Nature* **2009**, *461*, 633–635. (c) Dong, V. M.; Fiedler, D.; Carl, B.; Bergman, R. G.; Raymond, K. N. *J. Am. Chem. Soc.* **2006**, *128*, 14464–14465.
- (9) (a) Rebek, J., Jr. *Angew. Chem., Int. Ed.* **2005**, *44*, 2068–2078. (b) Rebek, J., Jr. *Acc. Chem. Res.* **2009**, *42*, 1660–1668.
- (10) Palmer, L. C.; Rebek, J., Jr. *Org. Biomol. Chem.* **2004**, *2*, 3051–3059.
- (11) For example: Liu, S.; Gan, H.; Hermann, A. T.; Rick, S. W.; Gibb, B. C. *Nat. Chem.* **2010**, *2*, 847–852.
- (12) (a) Chen, J.; Körner, S.; Craig, S. L.; Rudkevich, D. M.; Rebek, J., Jr. *Nature* **2002**, *415*, 385–386. (b) Chen, J.; Körner, S.; Craig, S. L.; Lin, S.; Rudkevich, D. M.; Rebek, J., Jr. *Proc. Natl. Acad. Sci. U.S.A.* **2002**, *99*, 2593–2596. (c) Gan, H.; Benjamin, C. J.; Gibb, B. C. *J. Am. Chem. Soc.* **2011**, *133*, 4770–4773. (d) O’Leary, B. M.; Szabo, T.; Svenstrup, N.; Schalley, C. A.; Lützen, A.; Schäfer, M.; Rebek, J., Jr. *J. Am. Chem. Soc.* **2001**, *123*, 11519–11533. (e) Liu, X.; Sun, J.; Warmuth, R. *Tetrahedron* **2009**, *65*, 7303–7310.
- (13) Heinz, T.; Rudkevich, D. M.; Rebek, J., Jr. *Nature* **1998**, *394*, 764–766.
- (14) Scarso, A.; Trembleau, L.; Rebek, J., Jr. *J. Am. Chem. Soc.* **2004**, *126*, 13512–13518.
- (15) Craig, S. L.; Lin, S.; Chen, J.; Rebek, J., Jr. *J. Am. Chem. Soc.* **2002**, *124*, 8780–8781.

- (16) For related phenomena with cycloalkanes and cavitands, see: (a) Gottschalk, T.; Jaun, B.; Diederich, F. *Angew. Chem., Int. Ed.* **2007**, *46*, 260–264. (b) Hornung, J.; Fankhauser, D.; Shirtcliff, L. D.; Praetorius, A.; Schweizer, W. B.; Diederich, F. *Chem.—Eur. J.* **2011**, *17*, 12362–12371.
- (17) Ajami, D.; Rebek, J., Jr. *J. Am. Chem. Soc.* **2006**, *128*, 15038–15039.
- (18) Ajami, D.; Rebek, J., Jr. *Nat. Chem.* **2009**, *1*, 87–90.
- (19) Eliel, E.; Wilen, S. H. *Stereochemistry of Organic Compounds*; Wiley: New York, 1994; p 600.
- (20) An alternate analysis, using the more popular 0.9 kcal mol<sup>-1</sup> value (vs 0.54–0.57 kcal mol<sup>-1</sup>) for a *gauche* effect, merely scales the value of the compensating C–H/ $\pi$  attractions as the difference, or about 0.35 kcal/mol. This represents the stabilization gained for a CH<sub>2</sub> brought closer to the aromatic panels induced by each *gauche* interaction. The value recommended by Nishio is 1.5–2.5 kcal mol<sup>-1</sup> for a C–H/ $\pi$  interaction: Nishio, M.; Hirota, M.; Umezawa, Y. In *The C–H/ $\pi$  interaction: Evidence, Nature, and Consequences. Stereochemistry of Organic Compounds*, Wiley-VCH: New York, 1998.
- (21) Barrett, E. S.; Dale, T. J.; Rebek, J., Jr. *J. Am. Chem. Soc.* **2007**, *129*, 8818–8824.
- (22) Wang, X.; Houk, K. N. *Org. Lett.* **1999**, *1*, 591–595.
- (23) Santamaria, J.; Martin, T.; Hilmersson, G.; Craig, S. L.; Rebek, J., Jr. *Proc. Natl. Acad. Sci. U.S.A.* **1999**, *96*, 8344–8347.
- (24) Dube, H.; Ajami, D.; Rebek, J., Jr. *Angew. Chem., Int. Ed.* **2010**, *49*, 3192–3195.
- (25) Lin, L.; Hale, S. P.; Schimmel, P. *Nature* **1996**, *384*, 33–34.